



CHAPTER 6

RESULTS AND DISCUSSION

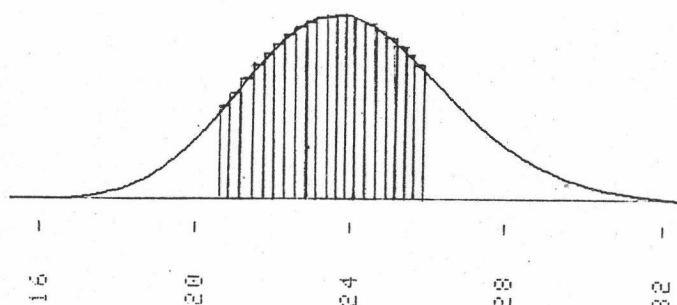
6.1 Evaluation of Moments of the chromatographic curves

Fig. 6.1 Chromatographic response

Fig. 6.1 shows an example of experimental chromatographic curves of the effluent from the adsorption column. In order to evaluate the first absolute and second central moments from equations (4.13) and (4.14), the observed deflection will be used in place of concentration because of the direct proportionality between the gas concentration and the deflection of the integrator connected with the ionization detector at the column outlet. The chromatographic curve is divided into smaller sliced area, as shown in Fig. 6.1, and the integrals were evaluated numerically from the chromatographic curve using Simpson's rule.

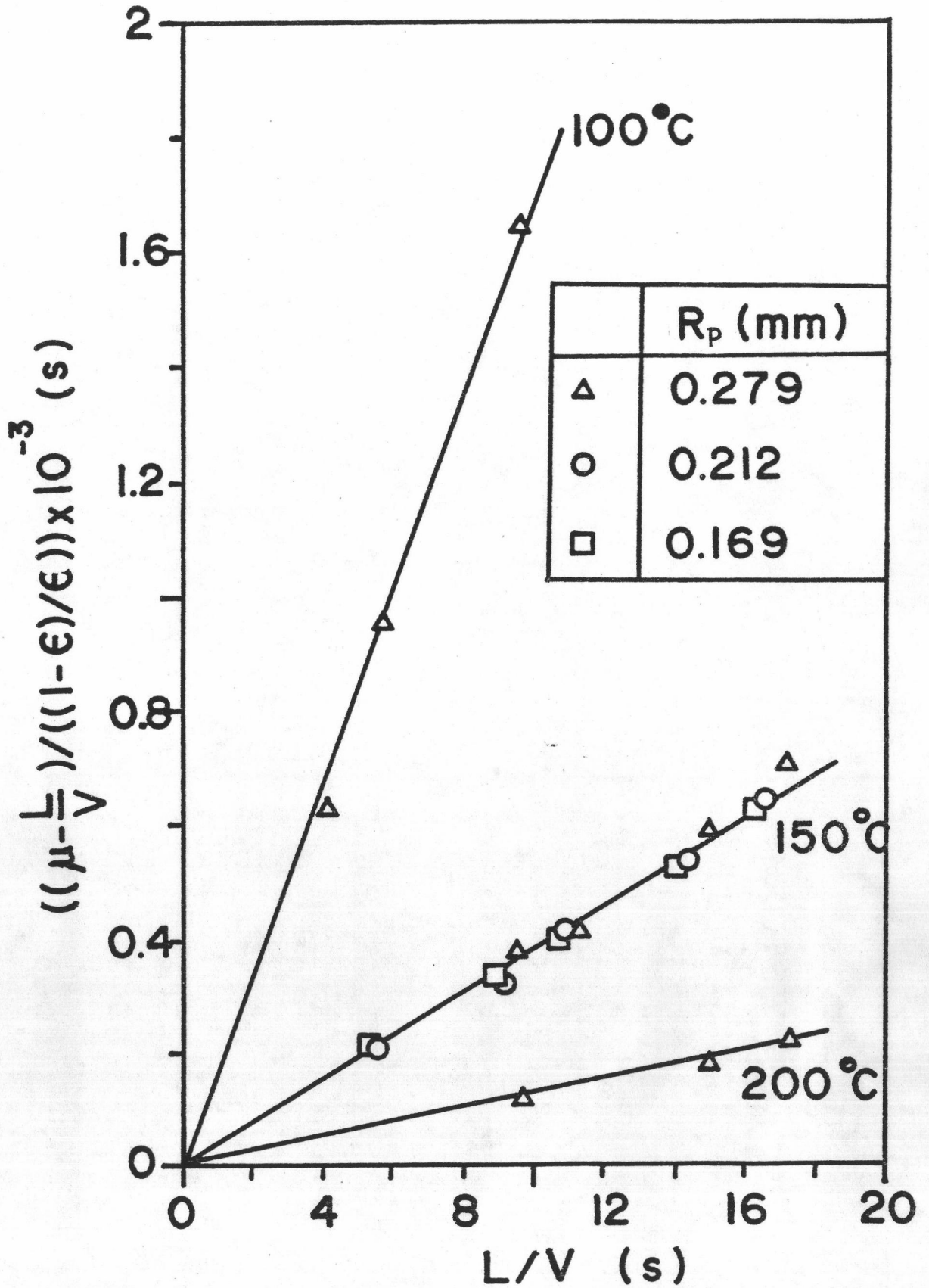


Fig. 6.2 Plot to calculate K_p from the first moment for the adsorption of n-Butane on NaY zeolite.

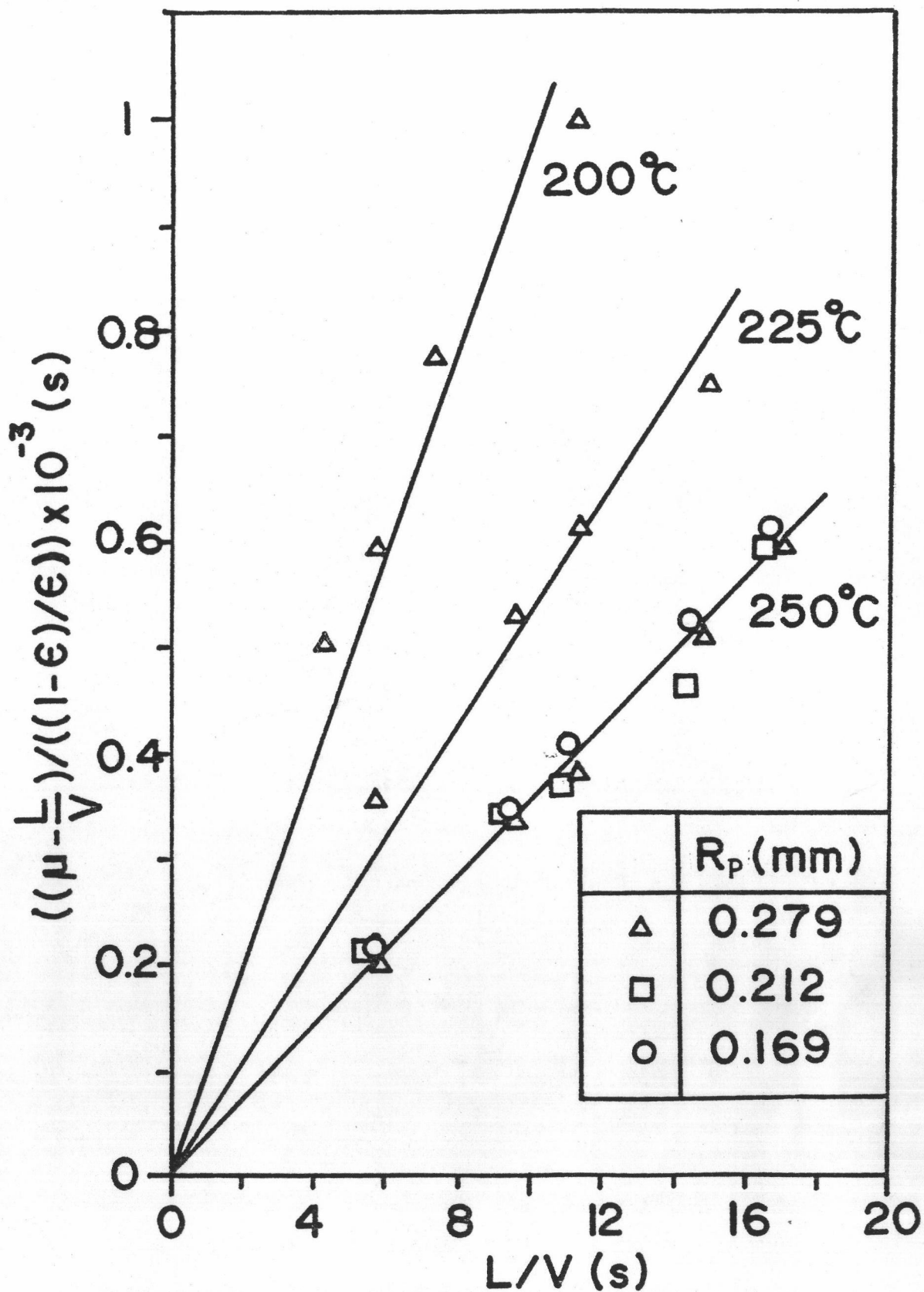


Fig. 6.3 Plot to calculate K_p from the first moment for the adsorption of n-Butane on Offretite/Erionite zeolite.

6.2 First moment Results

From equation (4.16), it follows that

$$\frac{\left(\mu - \frac{L}{v} \right)}{\left(\frac{\epsilon}{1-\epsilon} \right)} = K_p \cdot \frac{L}{v} \quad (6.1)$$

Plots of the reduced moment (the left side of the equation) versus L/v with the slope, K_p , are shown in Fig. 6.2 and 6.3 for the adsorption of n-butane on NaY and Offretite/Erionite zeolites. The linearity of the plots indicates that in the range of flow rates used (0-3 cm/s) K_p is independent of the flow rate of the gas through the adsorption column. At constant temperature, data for different sizes of zeolite particles (i.e., $R_p = 0.169, 0.212,$ and 0.279 mm) fall on the same straight line for both zeolites. The particle size therefore has no effect on K_p or the adsorption equilibrium of the system. Consequently, such plots are extended to various temperatures by using only one particle size, $R_p = 0.279$ mm (see Fig. 6.2 and 6.3).

The values of K_p , adsorption equilibrium constant for an adsorbent particle, obtained can be used to calculate K_c , adsorption equilibrium constant for a crystal, according to equation (4.18). Table 6.1 and 6.2 show the values of K_p and K_c , the adsorbed amount on both zeolites, decrease with increasing temperature. Furthermore, at the same temperature ($T = 200^\circ\text{C}$) K_p and K_c values for Offretite/Erionite zeolite are greater than those for NaY zeolite. This indicates the higher adsorption ability of Offretite/Erionite, which is due to its smaller pore size compared to NaY zeolite. The change in K_c with temperature can be correlated by the Van't Hoff equation to obtain the isosteric heat of adsorption, ΔH_0

Table 6.1 Equilibrium adsorption constant for NaY zeolite.

T (°C)	K_p (-)	K_c (-)
100	167.79	252.95
150	38.38	57.46
200	13.04	19.18

$$-\Delta H_0 \text{ for NaY zeolite} = -9.01 \text{ kcal/mol.K}$$

Table 6.2 Equilibrium adsorption constant for Offretite/Erionite zeolite.

T (°C)	K_p (-)	K_c (-)
200	96.86	153.21
225	53.36	84.14
250	35.27	55.41

$$-\Delta H_0 \text{ for Offretite/Erionite zeolite} = -9.98 \text{ kcal/mol.K}$$

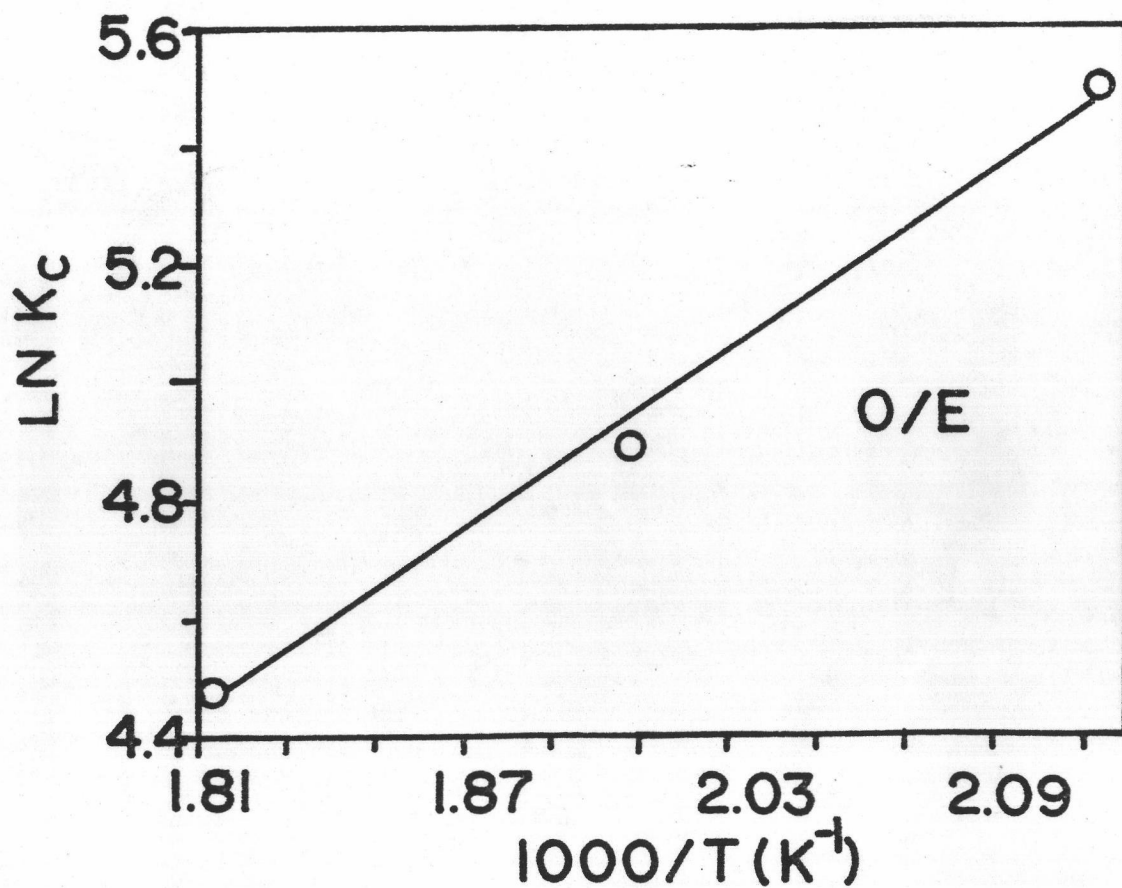
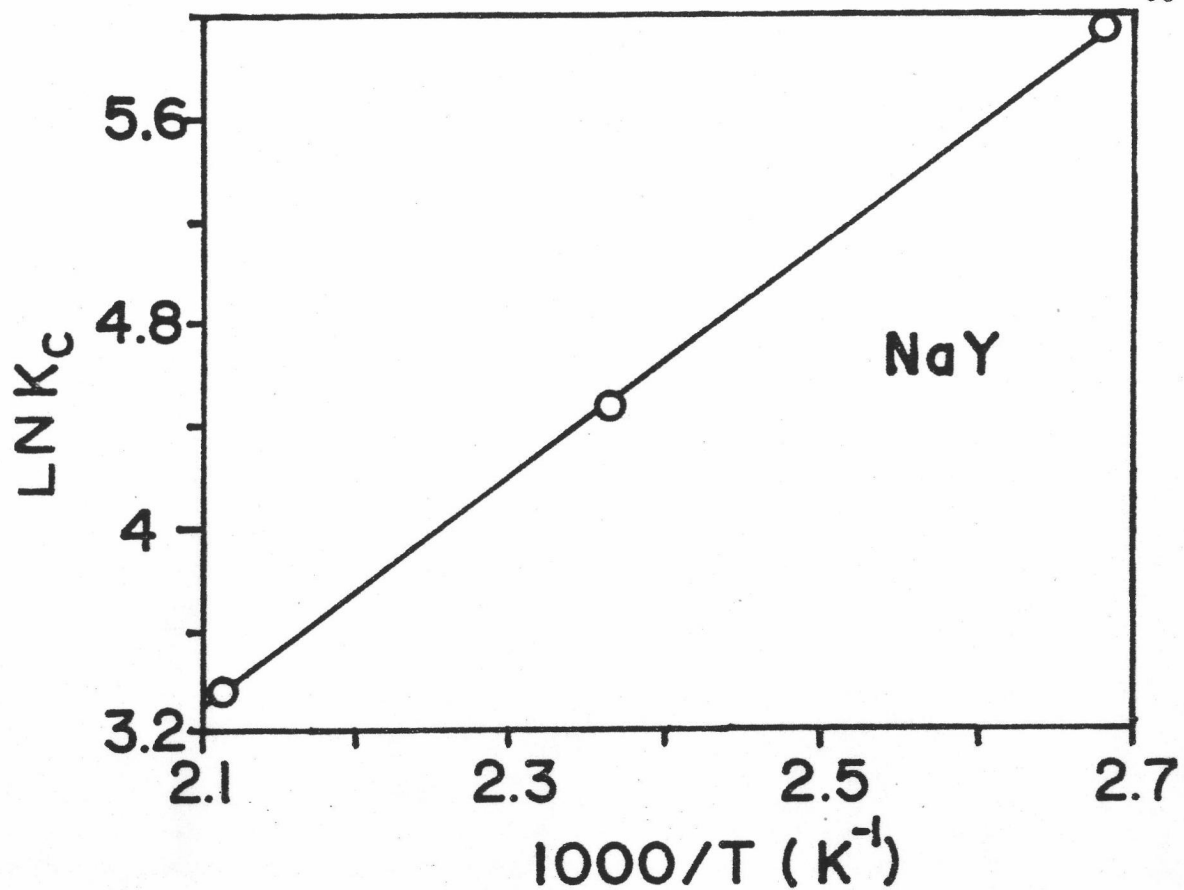


Fig. 6.4 Plot to calculate the heat of adsorption for the adsorption of n-Butane on NaY and Offretite/Erionite zeolite.

$$K_C = K_0 \exp(-\Delta H_0/RT) \quad (6.2)$$

$$\text{or} \quad \ln K_C = \ln K_0 + (-\Delta H_0/RT) \quad (6.3)$$

From equation (6.3), ΔH_0 can be obtained from the plot between $\log K_C$ versus $1/T$ given in Fig. 6.4. The results indicate the heat of adsorption of -9.01 kcal/mol.K and -9.98 kcal/mol.K for the adsorption of n-butane on NaY and Offretite/Erionite zeolites respectively. The smaller heat of adsorption for NaY zeolite can be explained by its three-dimensional structure and larger pore opening which is easier to travel in compared to Offretite/Erionite zeolite with its two-dimensional structure and smaller pore size. The heat of adsorption for n-butane sorption in NaY zeolite has also been reported (12) of 8.9 kcal/mol.K which agrees well with this study.

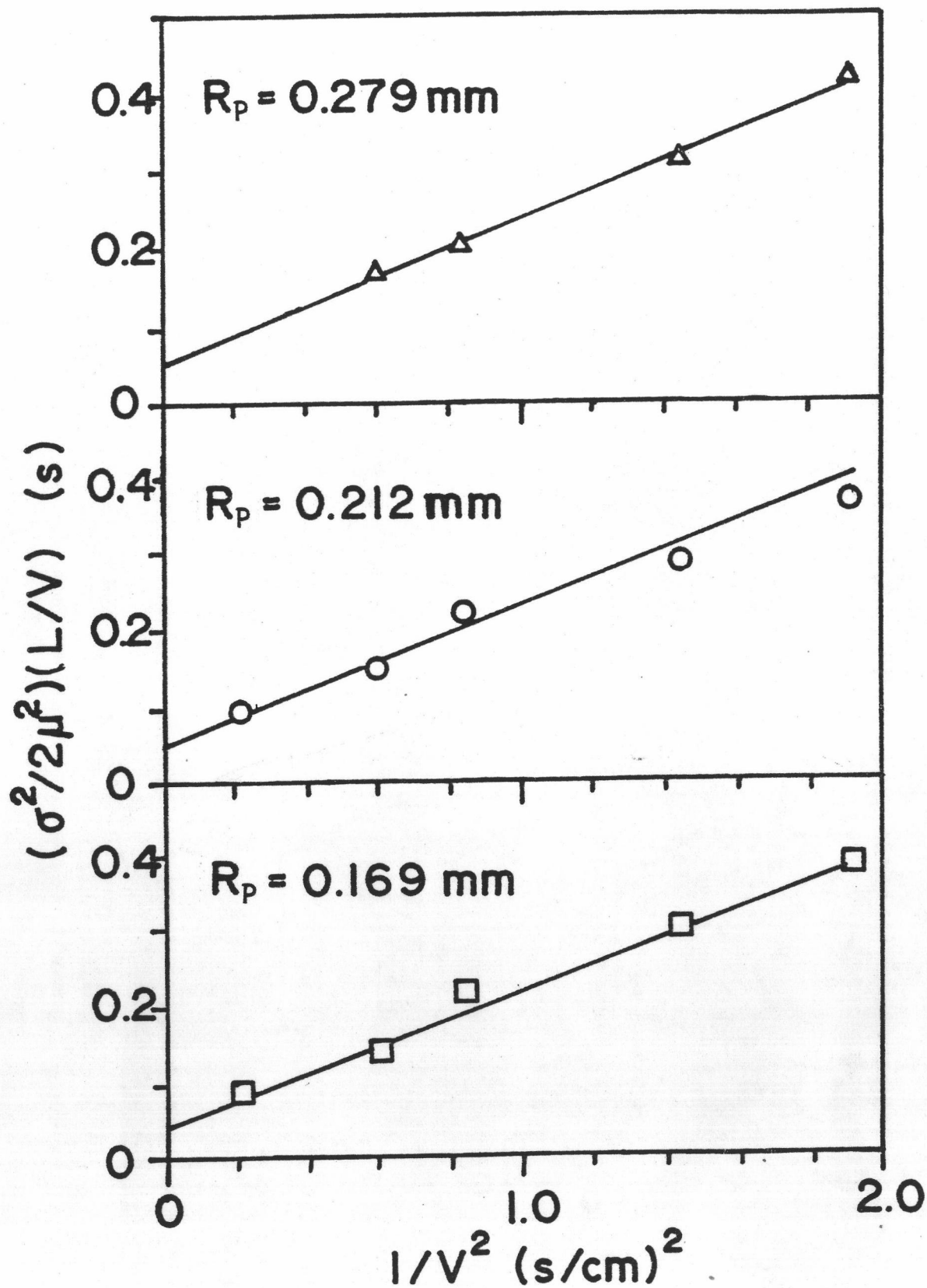


Fig. 6.5 Plot to calculate D_L from the second moment for the adsorption of n-Butane on NaY zeolite.

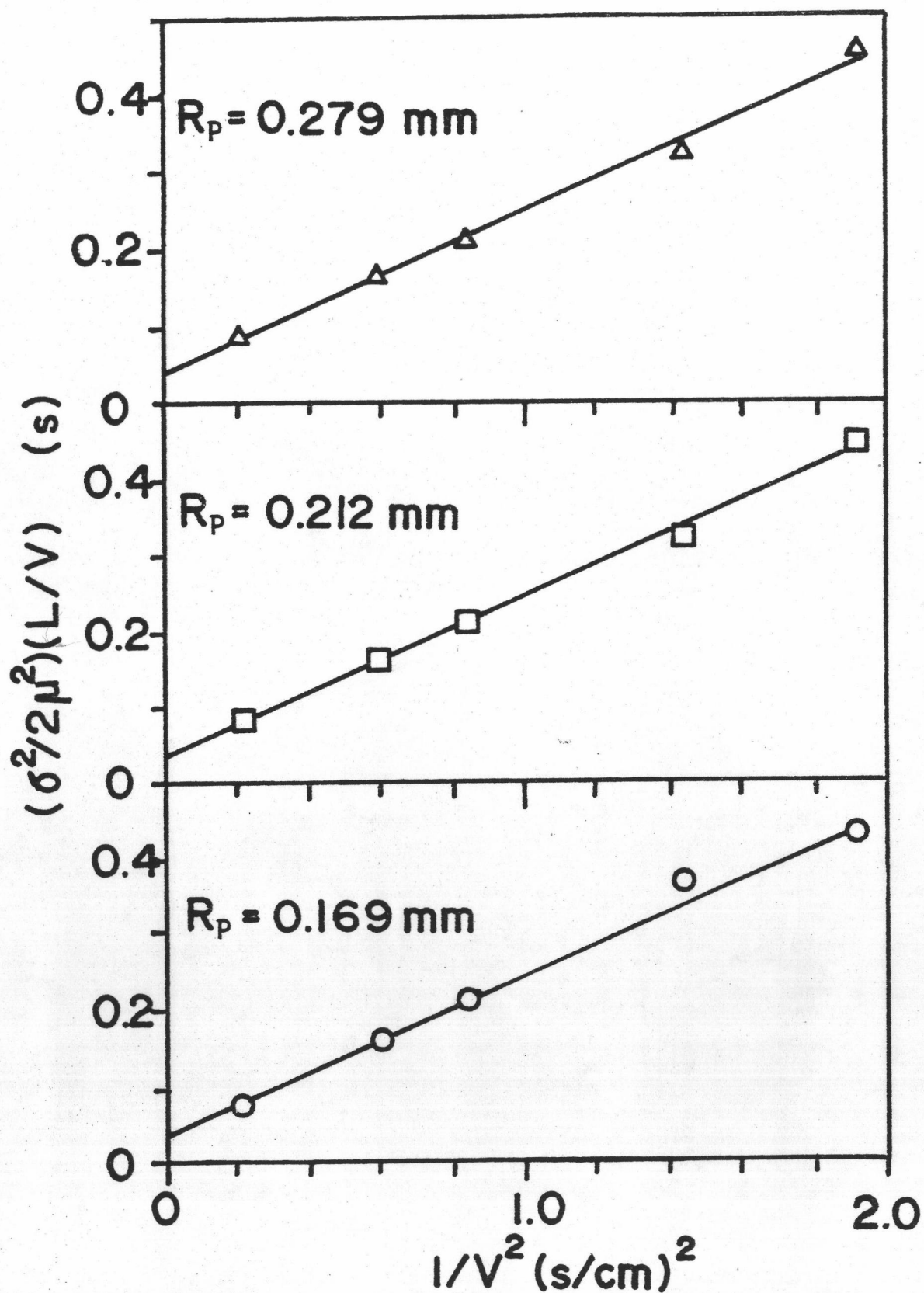


Fig. 6.6 Plot to calculate D_L from the second moment for the adsorption of n-Butane on Offretite/Erionite zeolite.

6.3 Second moment results

Fig. 6.5 and 6.6 show plots of $(\sigma^2/2\mu^2)(L/v)$ versus $1/v^2$ which give the straight lines with their slopes of axial dispersion and intercepts corresponding to the total mass transfer resistance. The axial dispersion coefficients, D_L , are summarized in Table 6.3 and 6.4. The independence of D_L on velocity, based on the linearity of plots at various velocities (0-3 cm/s), and particle size, as seen in the tables, indicate that the axial dispersion can be assumed to be due only to molecular diffusion in the interparticle space. The external tortuosity factors, τ , defined by the following equation.

$$D_L = D_m / \tau \quad (6.4)$$

This definition supposes that the void structure of the bed of adsorbent can be represented by a parallel assembly of cylindrical capillaries of the same average diameter running in the direction of the gas flow. The tortuosity factor expresses the average length of the path followed by the flowing gas, relatively to the length of the bed. From the tables, τ are seen to decrease with increasing particle size. This is due to increasing void volume which at the same time decreases the external tortuosity and ease the diffusion path in the packed column.

According to equation (4.19), the intercepts of the lines in Fig. 6.5 and 6.6 can be related to macropore and crystal diffusivities.

$$\text{intercept} = \frac{\epsilon}{(1-\epsilon)} \left(\frac{R_p^2}{3D_m} + \frac{R_p^2}{15\theta D_p} + \frac{r_c^2}{15K_p D_c} \right) \quad (6.5)$$

From this equation, the intercepts are plotted with the square of the

Table 6.3 Axial dispersion coefficient for NaY zeolite
at $T = 150^{\circ}\text{C}$ and $D_m = 0.58 \text{ cm}^2/\text{s}$.

R_p (mm)	D_L (cm^2/s)	τ (-)
0.169	0.180	3.22
0.212	0.183	3.169
0.279	0.185	3.135

$$D_{L,ave} = 0.1826 \quad \tau_{ave} = 3.1746$$

Table 6.4 Axial dispersion coefficient for Offretite/Erionite zeolite
at $T = 250^{\circ}\text{C}$ and $D_m = 0.828 \text{ cm}^2/\text{s}$.

R_p (mm)	D_L (cm^2/s)	τ (-)
0.169	0.2092	3.957
0.212	0.2098	3.946
0.279	0.2100	3.942

$$D_{L,ave} = 0.2096 \quad \tau_{ave} = 3.948$$

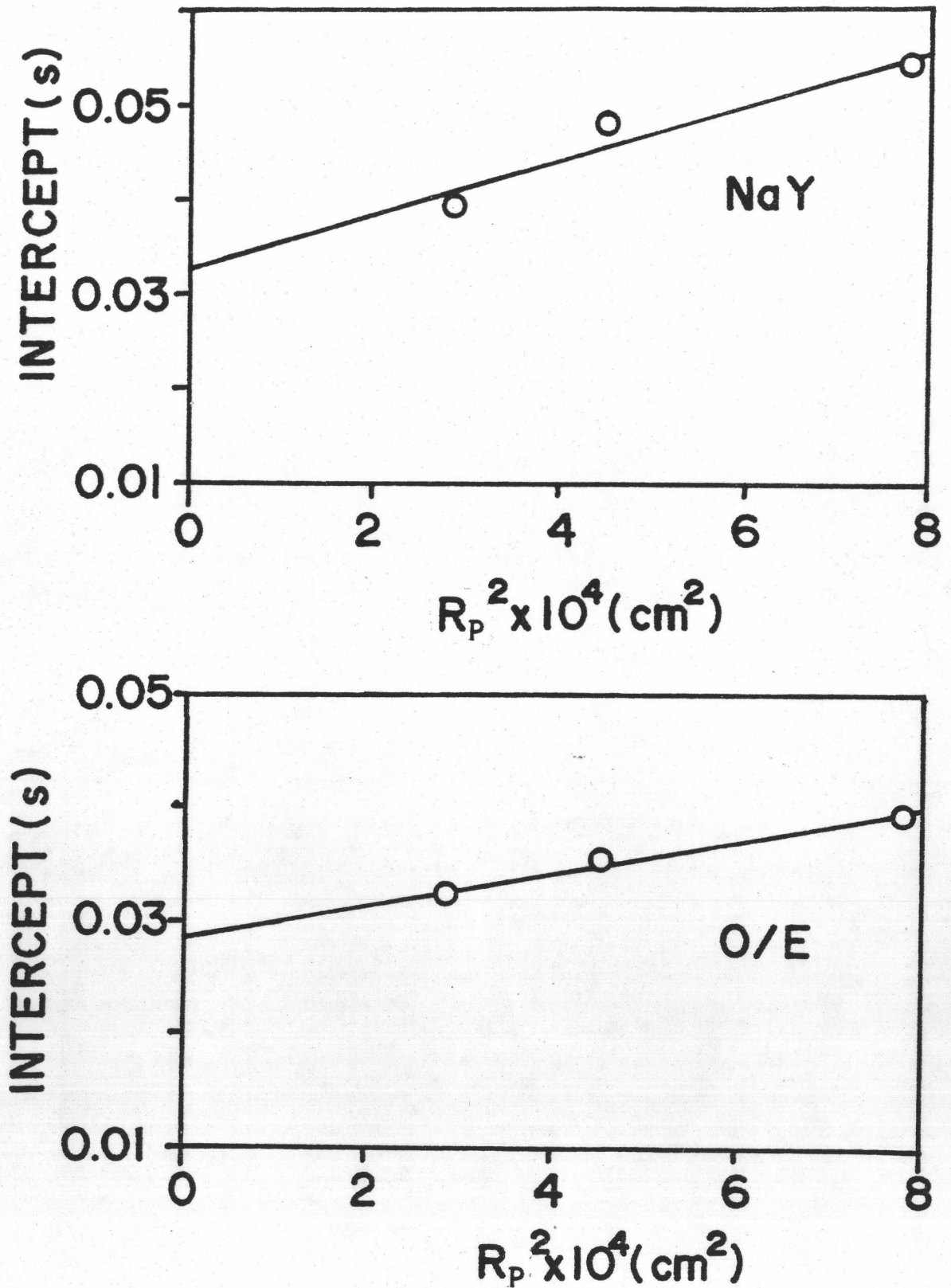


Fig. 6.7 Plot to calculate D_c for the adsorption of n-Butane on NaY NaY and Offretite/Erionite zeolite.

Table 6.5 Macropore diffusivity for NaY zeolite
at $T = 150^{\circ}\text{C}$.

R_p (mm)	$D_p \times 10^3$ (cm^2/s)
0.169	3.87
0.212	4.157
0.279	4.353

$$D_{p,ave} = 4.126$$

Table 6.6 Macropore diffusivity for Offretite/Erionite zeolite
at $T = 250^{\circ}\text{C}$.

R_p (mm)	$D_p \times 10^3$ (cm^2/s)
0.169	9.17
0.212	9.66
0.279	9.75

$$D_{p,ave} = 9.526$$

Table 6.7 Crystal diffusivity for NaY zeolite
at $T = 150^{\circ}\text{C}$.

R_p (mm)	$D_c/r_c^2 \times 10^2$ (s^{-1})
0.169	2.96
0.212	3.17
0.279	3.31

$$D_c/r_c^2, \text{ave} = 3.147$$

Table 6.8 Crystal diffusivity for Offretite/Erionite zeolite
at $T = 250^{\circ}\text{C}$.

R_p (mm)	$D_c/r_c^2 \times 10^2$ (s^{-1})
0.169	4.61
0.212	4.85
0.279	4.89

$$D_c/r_c^2, \text{ave} = 4.783$$

dispersion term outside the adsorbent particle, and the overall mass transfer term of the particle. From table 6.12, it is clear that the increasing temperature causes the overall mass transfer to increase whereas decreases the axial mixing inside the column. Therefore, the overall rate coefficient is seen to increase with increasing column temperature in Table (c). From comparison of k' of two zeolites, it is clear that the overall mass transfer rate inside NaY zeolite is higher than Offretite/Erionite zeolite at the same temperature ($T = 200^{\circ}\text{C}$). This follows the three-dimensional structure and larger pore size of NaY zeolite which is easier for mass transfer to occur than the two-dimensional structure and smaller pore size of Offretite/Erionite zeolite.

Table 6.9 Overall effective rate coefficient for NaY zeolite.

(a) Effect of particle size ($T = 150^{\circ}\text{C}$, $v = 1.09 \text{ cm/s}$)

R_p (mm)	$k' \times 10^2$ (s^{-1})
0.169	6.71
0.212	7.19
0.279	7.71

(b) Effect of flow rate ($T = 150^{\circ}\text{C}$, $R_p = 0.279 \text{ mm}$)

v (cm/s)	$k' \times 10^2$ (s^{-1})
0.72	3.78
0.83	5.02
1.09	7.71
1.30	9.38

(c) Effect of temperature ($v = 1.30 \text{ cm/s}$, $R_p = 0.279$)

T ($^{\circ}\text{C}$)	$k' \times 10^2$ (s^{-1})
100	2.19
150	9.38
200	21.91

Table 6.10 Overall effective rate coefficient for Offretite/Erionite zeolite.

(a) Effect of particle size ($T = 250^{\circ}\text{C}$, $v = 1.09 \text{ cm/s}$)

R_p (mm)	$k' \times 10^2$ (s^{-1})
0.169	9.12
0.212	10.04
0.279	10.19

(b) Effect of flow rate ($T = 250^{\circ}\text{C}$, $R_p = 0.279 \text{ mm}$)

v (cm/s)	$k' \times 10^2$ (s^{-1})
0.72	4.67
0.83	6.56
1.09	10.19
1.30	12.68

(c) Effect of temperature ($v = 1.30 \text{ cm/s}$, $R_p = 0.279$)

T ($^{\circ}\text{C}$)	$k' \times 10^2$ (s^{-1})
200	3.16
225	6.24
250	10.19

6.4 Overall rate of adsorption

The overall rate of adsorption here is determined in terms of the overall effective rate coefficient, k' . From equation (4.19), the coefficient can be defined (17)

$$\frac{1}{Kk'} = \frac{\sigma^2}{2\mu^2} \cdot \frac{L}{v} \left(\frac{1-\epsilon}{\epsilon} \right) = \frac{D_L}{v^2} \left(\frac{1-\epsilon}{\epsilon} \right) + \frac{R_p^2}{3D_m} + \frac{R_p^2}{15\epsilon_p D_p} + \frac{r_c^2}{15K_p D_c} \quad (6.6)$$

According to this equation, k' can be calculated from the first and second moments of the chromatographic curves. Table (6.9) and (6.10) show the values of k' for the adsorption of n-butane on NaY and Offretite/Erionite zeolites affected by the particle size, flow rate, and the temperature.

At constant temperature, the overall rate coefficient increases with increasing particle size, as seen from Table (a). Table 6.11 shows comparison of the relative contributions of axial dispersion, film plus macropore diffusional resistance and crystal diffusional resistance to the overall rate coefficient. It is apparent that as the particle size increases the contribution of axial dispersion and crystal diffusion increase whereas that of film plus macropore diffusion decrease. Furthermore, the overall rate is controlled by the axial dispersion under experimental condition.

From Table (b), the effect of flow rate in increasing k' may be clearly seen in axial dispersion term compared to the other terms, according to equation (6.6). Therefore, the increasing flow rate will influence the turbulent mixing inside the column and accordingly increase the overall rate coefficient of the system.

In viewing the effect of temperature, the overall rate coefficient, k' , may be separated into two terms, the axial

Table 6.11 Effect of particle size on k'

1. For NaY zeolite, at $T = 150^\circ\text{C}$ and $v = 1.09$ cm/s

R_p (mm)	$\frac{D_L}{v^2} \left(\frac{1-\epsilon}{\epsilon} \right)$ (s)	$\frac{R_p^2}{3D_m} + \frac{R_p^2}{15\theta D_p}$ (s)	$\frac{r_c^2}{15K_p D_c}$ (s)
0.169	0.273	0.0147	0.05868
0.212	0.259	0.0216	0.05479
0.279	0.249	0.0357	0.05247

2. For Offretite/Erionite zeolite, at $T = 250^\circ\text{C}$ and $v = 1.09$ cm/s

R_p (mm)	$\frac{D_L}{v^2} \left(\frac{1-\epsilon}{\epsilon} \right)$ (s)	$\frac{R_p^2}{3D_m} + \frac{R_p^2}{15\theta D_p}$ (s)	$\frac{r_c^2}{15K_p D_c}$ (s)
0.169	0.252	0.0057	0.0410
0.212	0.240	0.0086	0.0390
0.279	0.238	0.0147	0.0386

Table 6.12 Effect of temperature on k'

1. For NaY zeolite, $R_p = 0.279$ and $v = 1.30$ cm/s

T (°C)	$\frac{D_L}{v^2} \left(\frac{1-\epsilon}{\epsilon} \right)$ (s)	$\left(\frac{R_p^2}{3D_m} + \frac{R_p^2}{15\theta D_p} + \frac{r_c^2}{15K_p D_c} \right)$ (s)
100	0.1404	0.1317
150	0.1734	0.1044
200	0.2088	0.0444

2. For Offretite/Erionite zeolite, $R_p = 0.279$ and $v = 1.30$ cm/s

T (°C)	$\frac{D_L}{v^2} \left(\frac{1-\epsilon}{\epsilon} \right)$ (s)	$\left(\frac{R_p^2}{3D_m} + \frac{R_p^2}{15\theta D_p} + \frac{r_c^2}{15K_p D_c} \right)$ (s)
200	0.1410	0.1857
225	0.1537	0.1466
250	0.1672	0.1111

radius of the adsorbent particle, R_p for the n-butane sorption in both zeolites, as shown in Fig. 6.7 . Then, D_p can be obtained from the slope of the plot and are presented in Table 6.5 and 6.6 . It is apparent that the macropore diffusivities of order 10^{-3} cm^2/s are too small to be approximated with molecular diffusion. Furthermore, D_p is rather constant and independent of particle size. Therefore, the possible mechanism of macropore diffusion may be Knudsen diffusion and perhaps includes surface diffusion.

Table 6.7 and 6.8 show the calculated values of D_c/r_c^2 from the intercept of the above plot, according to equation (6.5). The particle size is seen to have no effect on the diffusion in zeolite crystal. Generally, the crystallite size of the commercial synthetic zeolite is in the range of 1-10 μm (17). Then the order of the crystal diffusivity for n-butane sorption in both zeolites can be approximated of 10^{-10} cm^2/s which is very slow compared to macropore diffusion and axial dispersion. Because of a very small crystallite size, the diffusion in crystal can be viewed as an activated process, involving the activation energy of the diffusing molecule, which depends on the crystal radius and the attraction force of the adsorbent surface.